Premelting and the hydrogen-exchange open state in synthetic RNA duplexes

ARTICLE *in* BIOPOLYMERS · NOVEMBER 1984

Impact Factor: 2.39 · DOI: 10.1002/bip.360231102 · Source: PubMed

Premelting and the Hydrogen-Exchange Open State in Synthetic RNA Duplexes

R. S. PREISLER, C. MANDAL, S. W. ENGLANDER, and N. R. KALLENBACH, *Departments of Biology, Biochemistry and Biophysics, University of Pennsylvania/G7, Philadelphia, Pennsylvania 19104*, and J. FRAZIER, H. T. MILES, and F. B. HOWARD, *Laboratory of Molecular Biology, NIMDD, National Institutes of Health, Bethesda, Maryland 20205*

Synopsis

Here we attempt to relate equilibrium temperature-dependent spectral changes in two synthetic RNA homopolymer duplexes—poly(rA) · poly(rU) and poly(rI) · poly(rC)—to the conformational opening detected in stopped-flow hydrogen–deuterium exchange experiments on these molecules. We are concerned with changes in several spectral properties that occur well below onset of the thermally induced helix-coil "melting" transition in these systems. These are known as "premelting" transitions, and can be detected in uv CD spectra as well as in vibrational bands of the bases in the ir. Both CD and ir spectra exhibit isoelliptic or isosbestic points consistent with a well-defined two-state premelting process. Application of a least-squares analysis to two-state models for premelting using data from different bands in the CD and ir shows that the enthalpies are substantially greater than that of the hydrogen-exchange opening. Thus the hydrogen-exchange open state represents only one premelting reaction among several that lead to equilibrium changes in helix geometry or base vibrational modes. The latter include processes that occur on a rapid time scale, including potential base-pair openings not productive for the exchange reaction. It appears that the former, and not the hydrogen-exchange opening, dominates the premelting alterations monitored by ir and CD spectroscopy.

INTRODUCTION

An understanding of the structural dynamics of nucleic acids at physiological temperatures and solution conditions is likely to be important in terms of the mechanisms of fundamental cellular events, such as DNA replication, recombination, or transcription. Over a number of years, the highly cooperative helix-coil transitions seen in DNA and synthetic polynucleotides[1] gave rise to a picture of the double helix as a static structure, which changes its conformation to a random-coil form only in the vicinity of the denaturation midpoint, T_m. This notion is at variance with several lines of experimental evidence indicating (1) that the double-helix backbone exhibits a range of large amplitude motions down to a time scale of nanoseconds,[2] and (2) that a number of physical and chemical properties of DNA and polynu-

Biopolymers, Vol. 23, 2099–2125 (1984)
 CCC 0006-3525/84/112099-27$04.00

cleotide duplexes change with temperature far below the onset of any detectable denaturation. These latter phenomena have been referred to as "premelting transitions"[3] to distinguish them from melting or global helix denaturation. Premelting changes in polarographic behavior,[4] CD,[5-11] Raman spectra,[12-14] and ^{31}P-nmr line shapes and chemical shifts,[2] have all been reported. The phenomenon in deoxypolynucleotides has been discussed in terms of gradual changes in helix parameters (winding angle or base twist[15]) without significant disruption of the double-stranded structure. As we show here, this description does not seem appropriate to the large-enthalpy premelting process in synthetic RNA duplexes studied here and in a previous publication.[16]

We have shown that hydrogen-exchange (HX) measurements on poly(rA) · poly(rU) provide evidence for the existence of an open state in this duplex in which 5% of the base pairs are broken at pH 7 and room temperature.[17] We have argued elsewhere that this opening does not lead to unstacking or internal "melting" (i.e., forming a small bubble) within the helix. Instead, what we refer to as the HX open state appears to involve a minimal torsional oscillation of the duplex that severs both H bonds in either poly(rA) · poly(rU) or poly(rI) · poly(rC) without loss of most of the stacking free energy. The extent of opening is lower in the latter helix (1% at room temperature), but poly(rI) · poly(rC) behaves similarly to poly(rA) · poly(rU) in other respects. (We refer to these homopolymer complexes here as "AU" and "IC," respectively.)

Given that a number of features of the polynucleotide duplex can be seen to depend on temperature in premelting, is this a manifestation of the same opening responsible for exposing base-pair protons to exchange? In order to answer this question, we have carried out an extended series of equilibrium spectroscopic measurements on the AU and IC duplexes over a temperature range of about 50°C below the T_m. We use CD to provide a probe of helix geometry as well as base-pairing present, since the interactions responsible are sensitive to both properties.[5-11] We use ir spectroscopy because, while it is relatively insensitive to base stacking in single-stranded polynucleotides, it is extremely sensitive to changes in conformation in hydrogen-bonded nucleic acids.[18] If premelting in these duplexes involves the kind of changes postulated for DNA, the CD and ir spectra might be expected to reveal distinctive thermal transition profiles. On the other hand, the ir measurement seems more likely to reflect conformational effects corresponding to the base-pair breaking required in HX opening. This work extends our preliminary observations reported previously.[16]

THEORY

We attempt here to compare the temperature dependence of the ir and CD spectra of A · U and I · C duplexes with that determined from

the HX rates, measured on the same samples, over the same range of temperatures (where possible). To answer the question raised above, or evaluate the hypotheses just considered, requires quantitative comparison of these properties. Consider a minimal two-state transition model

$$A \rightleftharpoons B$$

for which K_{eq} denotes the equilibrium constant, and let α be a parameter responsive to the difference between A and B. Then at temperature, T

$$\ln K_{eq} = \ln\left(\frac{\alpha_A - \alpha}{\alpha - \alpha_B}\right) = \frac{\Delta S^0}{R} - \frac{\Delta H^0}{RT} \tag{1}$$

Here, α_A and α_B are the values of the intensity or frequency of a spectral band (for example) which describe a set of molecules entirely in the A or B state. ΔH^0 and ΔS^0 are the van't Hoff enthalpy and entropy, respectively, for the transition.[19] Our objective is to try to determine K_{eq} from sets of temperature-dependent CD or ir spectral data, and to relate these to the analogous results from HX kinetics.

Determining the temperature dependence of the equilibrium constant is straightforward from the hydrogen exchange.[17] The model for opening-dependent hydrogen exchange is

$$H_{closed} \rightleftharpoons H_{open} \rightarrow H_{exchanged} \tag{2}$$

where a proton cannot exchange in the native duplex (or closed) state, but can exchange following a conformational change to an open state. The reference states A and B, for closed and open base pairs, respectively, are experimentally observable or theoretically definable. Thus, K_{eq} can be computed from the first equality in Eq. (1). Measuring K_{eq} at several temperatures leads to the van't Hoff enthalpy ΔH^0.

The calculation of enthalpies for spectroscopically measured premelting is, by comparison, problematical. Since we do not now what sort of conformational change is detected by ir or CD, we are unable to define "nonpremelted" and "fully premelted" reference states or predict their spectral properties. In terms of Eq. (1), we do not know α_A and α_B.

In order to calculate values of K_{eq} and ΔH^0 from spectroscopic data, we first tried a least-squares computer-fitting scheme (Program I) based on the method of Powell et al.[19] The program is given a range of guesses of ΔH^0 and $T_m = \Delta H^0/\Delta S^0$. From each pair of these parameters, it calculates values of the equilibrium constant and fits values of α_A and α_B to provide trial values of the spectroscopic values,

α_i^*, to be compared with the experimental values, α_i at each temperature, T_i. The combination of ΔH^0 and T_m values that minimize the sum

$$S = \sum_i (\alpha_i^* - \alpha_i)^2 \tag{3}$$

is selected.

For most of our spectroscopic data sets, the program failed to find a minimum over a wide range of ΔH^0 and T_m values. Therefore, we modified the program to include a normalizing assumption.[16] The values of K_{eq} at 20°C were arbitrarily set to the equilibrium constant derived from HX kinetic data for that temperature, 0.05 for AU and 0.01 for IC. With this constraint, the T_m becomes a function of ΔH^0 and enthalpy values are the only input. The modified program (II) found minima for a larger number, but still not all, of the spectroscopic data sets.

Those spectroscopically derived enthalpies of which we are reasonably confident lie predominantly in a range from two to three times the values from the HX-rate experiments. Thus, if ir is measuring the same open state as HX, the former technique must also be detecting substantial additional conformational changes which do not affect exchange rates. The kinds of premelting effects that have been invoked to explain CD spectral changes in DNA should have a smaller enthalpy than base-pair opening, provided that units of equal size are involved in each case. The fact that in RNA the CD premelting enthalpies are larger than those from HX indicates either a larger transition "unit" or a process different from the one suggested for DNA.

MATERIALS AND METHODS

Polyadenylic [poly(rA)], polyuridylic [poly(rU)], polyinosinic [poly(rI)], and polycytidylic [poly(rC)] acids were purchased from P-L Biochemicals. Solutions of individual polymers were extensively dialyzed to remove small contaminating fragments. Polymer sizes were determined by electrophoresis on 8*M* urea, 10% acrylamide gels to be larger than 100 nucleotides. Concentrations were determined by uv absorption in a Perkin–Elmer 552 spectrophotometer. The following molar extinction values (M^{-1}/cm) were used: poly(rA), 10,400 at 257 nm; poly(rU), 9900 at 260 nm; poly(rI), 10,260 at 248 nm; and poly(rC), 6300 at 268 nm.[20,21] The 1:1 complexes, AU and IC, were prepared by mixing the polymer solutions in the mass ratios that gave equimolarity. Each mixture was heated to denaturing temperature and allowed to cool slowly to ensure complete renaturation.

Kinetic properties of base-pair opening reactions were measured in an OLIS stopped-flow spectrophotometer system equipped with a Bausch and Lomb monochromator and an observation cell, photomultiplier, and mixing system from Durrum. The instrument was in-

terfaced to a NOVA2 computer, using OLIS software. Each polynucleotide complex in D_2O solution was mixed with nine volumes of H_2O buffer, and the resulting small decrease in optical density around 290 nm (arising from a red shift in the kinetic difference spectrum) was monitored on as many as three different time scales.[17]

Infrared spectra in D_2O were measured in 26- or 54-μm CaF_2 cells in a Perkin–Elmer 580B spectrophotometer, with temperature regulated by a circulating water bath. CD spectra in H_2O were recorded, using 1 cm quartz cuvets, with a Jasco J500A spectrometer, regulated with a Lauda bath. Both ir and CD instruments were interfaced to Dec 1103 computers which transmitted data to a Honeywell 516 at NIAMDD for processing. Programs I and II were run on the PDP-10 computer system at the University of Pennsylvania School of Medicine.

RESULTS

Kinetics of Hydrogen–Deuterium Exchange

A time-dependent uv spectral shift is produced by exchanging deuterons on the base chromophores of AU and IC with solvent protons. The time course of this process, monitored at the peaks of the respective H–D kinetic difference spectra (290 nm for AU; 293 nm for IC) can be analyzed according to two first-order processes. Figure 1 shows Arrhenius plots for the fast and slow rates observed with both complexes, measured between 10 and 40°C in AU and between 15 and 35°C in IC.

Detailed studies of hydrogen–deuterium exchange (HX) in AU and its component monomers and polynucleotides[17] allow the fast reaction to be assigned to the uracil N-3 imino proton and the slow reaction to the two exocyclic amino protons of adenine (Fig. 2). Although only one of the two amino protons is involved in interbase hydrogen bonding while the other is exposed to the solvent, they exchange at the same rate. Because of the high basicity of the amino group in the unmodified base, the exchange process near neutral pH proceeds via prior protonation of the adenine ring N-1, which is also hydrogen bonded in the duplex. Finally, the uracil imino proton participates in Watson–Crick base pairing as well, and is buried in the double helix. These observations lead to the conclusion that exchange of the three protons with solvent requires base-pair breakage or opening.

The imino proton of uracil exchanges by a direct transfer to solvent OH^- more rapidly than the reclosing of the base pair. Since this reaction accompanies every base-pair breakage, the rate of the fast phase is equivalent to the rate of helix opening. Thus, according to the data plotted in Figure 1, AU opens with a rate constant of 1.1 s^{-1} ($t_{1/2}$ = 630 ms) at 20°C.

The adenine amino protons exchange through a preequilibrium

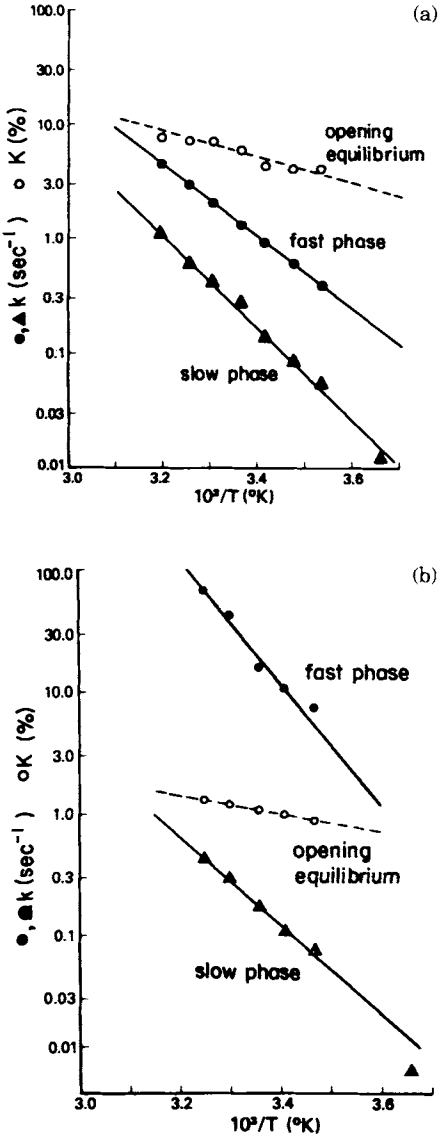

Fig. 1. Temperature-dependence of hydrogen-exchange kinetics and the base-pair-opening equilibrium: (a) poly(rA) · poly(rU); (b) poly(rI) · poly(rC). Kinetic data were obtained in 100 m*M* NaCl, 10 m*M* NaH_2PO_4, pH 7.0, with a computer-interfaced stopped-flow spectrophotometric system. Rate constants for exchange, k_{ex}, are represented in an Arrhenius plot of ln k_{ex} vs $1/T$. Opening equilibrium constant, K_{op}, was calculated as described in Results. These data are represented in a van't Hoff plot of ln K_{op} vs $1/T$.

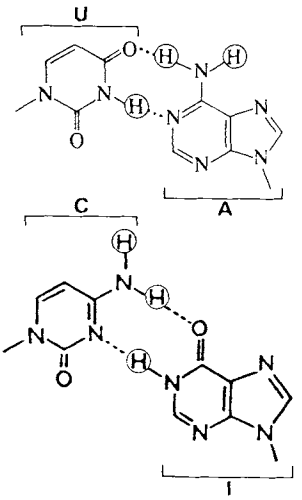

Fig. 2. Exchangeable protons in A:U and I:C base pairs. Exchange of the circled hydrogens with solvent is detected with the stopped-flow spectrophotometric technique.

mechanism from the transiently open base pair. This process is sensitive to pH and general base catalysis under the same conditions affecting exchange of the amino protons in single-stranded poly(rA) or monomer AMP. Either of these component moieties of AU can be used to represent the 100% open reference state. Poly(rA), which is considerably stacked at room temperature, is the appropriate choice if the open state is assumed to retain stacking of the adenine base with its nearest neighbors (as in the minimal model presented in Ref. 17). AMP, on the other hand, would be a better reference for a model in which the open state involves unstacking of the adenine.

Although a different expression has been derived from the specific model for open-limited hydrogen exchange,[17] Eq. (1) can be applied to determining the equilibrium constant for base pair opening, K_{op}. In this example, the observed parameters are the temperature-dependent exchange rate constants k_{ex} of the slow phase (amino exchange) in AU. State A is the theoretical fully closed helix, where the rate constant for amino exchange, is zero. Using kinetic data from 20°C and poly(rA) for state B, we calculate

$$K_{op} = \frac{\alpha_A - \alpha}{\alpha - \alpha_B} = \frac{k_{ex}(\text{closed}) - k_{ex}(\text{AU})}{k_{ex}(\text{AU}) - k_{ex}[\text{poly(rA)}]}$$

$$= \frac{(0.0 - 0.14)\ \text{s}^{-1}}{(0.14 - 3.1)\ \text{s}^{-1}} = 0.05$$

The result with AMP as the fully open standard is given in Table I.

We have recently performed a similar investigation of HX in IC,

TABLE I
Kinetic and Thermodynamic Parameters of Hydrogen Exchange and Base-Pair Opening[a]

Property	Poly(rA):Poly(rU)	Poly(rI):Poly(rC)
k_{ex} (fast phase) (s^{-1} at 20°C)	1.1	12
k_{ex} (slow phase) (s^{-1} at 20°C)	0.14	0.13
Polynucleotide Standard		
K_{op} (at 20°C)	0.05	0.01
ΔH^0 (kcal/mol)	3.8	3.7
ΔS^0 (cal/mol K)	6.7	3.3
T_m (°C)	290	840
Mononucleotide Standard		
K_{op} (at 20°C)	0.02	0.004
ΔH^0 (kcal/mol)	6.1	6.3
ΔS^0 (cal/mol K)	12	2.5
T_m (°C)	240	360

[a] Kinetic measurements were performed in 100 m*M* NaCl, 10 m*M* NaH_2PO_4, pH 7.0.

details of which will be published elsewhere. We conclude that the fast reaction (Fig. 1) corresponds to exchange of the N-1 imino proton in hypoxanthine and the slow process involves the two exocyclic C-4 amino protons of cytosine (Fig. 2). As in AU, two out of three exchangeable protons participate in base pairing in the duplex, implying that exchange is dependent on opening. Nakanishi and Tsuboi[22] have reported similar exchange rates in IC. They originally assigned the fast reaction to the nonhydrogen-bonded cytosine amino proton and the slow reaction to the hypoxanthine imino and hydrogen-bonded cytosine amino protons. This interpretation is inconsistent with the HX behavior of component monomers and polymers,[17] as well as with our data on the pH dependence of exchange in IC, and has since been retracted.

The hypoxanthine imino proton exchanges in a direct, conformationally dependent manner analogous to the uracil imino proton in

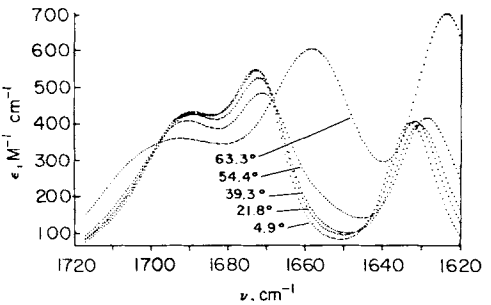

Fig. 3. Infrared spectra of poly(rA):poly(rU) at different temperatures. Solvent was D_2O, 100 m*M* NaH_2PO_4, pD 7. Data are corrected for a slight drift in baseline (between 1800 and 1750 cm^{-1}) with temperature.

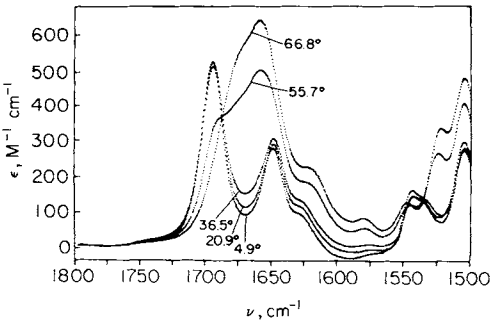

Fig. 4. Infrared spectra of poly(rI):poly(rC) at different temperatures. Conditions and corrections were the same as those described in the legend to Fig. 3.

AU. Thus, the rate constant for the fast phase in IC measures the opening of the helix, which occurs at 12 s^{-1} ($t_{1/2}$ = 58 ms) at 20°C (Fig. 1). The cytosine amino protons exchange via the same sort of preequilibrium opening-dependent mechanism, with prior protonation at N-3 in cytosine, as was previously described for the adenine protons in AU. Thus, K_{op} for IC can be calculated from the rate constant of the slow phase, with reference either to poly(rC) or CMP. The results are listed in Table I.

Van't Hoff plots (ln K_{op} vs $1/T$) for base-pair opening in AU and IC are included in Figure 1. In the form

$$\ln K_{eq} = -(\Delta H^0/R)\,(1/T) + \Delta S^0/R \tag{4}$$

the enthalpy can be calculated from the slope and entropy from the y intercept of these graphs.

At $T = T_m$, the two states involved in the transition are at equal concentration, and $K_{eq} = 1$. Thus from Eq. (4)

TABLE II
Assignments of IR Absorption Bands[a]

Poly(rA):Poly(rU)			Poly(rI):Poly(rC)		
5°C	70°C	Assignment	5°C	70°C	Assignment
Frequency (cm^{-1})					
1569	1576	A-ring	1505	1505	C-ring (I-ring)[b]
1633	1624	A-ring	1543	1522	C-ring (I-ring)[b]
1673	1658	U-C4 carbonyl	1648	1659	C-carbonyl
1689	1692	U-C2 carbonyl	1695		I-carbonyl

[a] Spectra were measured in D_2O, 100 mM NaCl, 1 mM NaH_2PO_4, pD 7. Assignments are based on information in Refs. 18 and 23.

[b] Smaller contributions in parentheses.

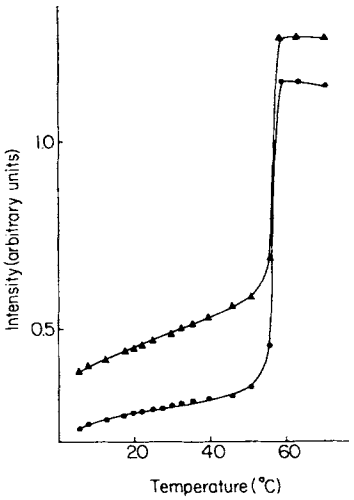

Fig. 5. Intensities of vibrational bands in poly(rA):poly(rU) as a function of temperature: (●) 1658.5 cm^{-1}, (▲) 1624.0 cm^{-1}. Baseline-corrected data. T_m for the helix-coil transition was estimated to be 57°C from the data at both frequencies. This value is in close agreement with the T_m determined from uv spectroscopy (Ref. 24).

$$\Delta H^0/RT_m = \Delta S^0/R \text{ or } T_m = \Delta H^0/\Delta S^0 \quad (5)$$

Values of enthalpy, entropy, and T_m for base-pair opening in AU and IC are given in Table I.

Premelting Changes in the IR and CD Spectra

Infrared spectra of AU and IC in D_2O, 0.1*M* NaCl, were measured at 18 different temperatures between 5 and 70°C. Selected spectra are plotted in Figures 3 and 4 and band assignments are given in Table II. Obvious premelting changes can be seen in both intensities (Figs. 5 and 6) and frequency (Fig. 7) of the vibrational bands in each complex. Isosbestic points for spectra covering the entire range of temperatures occur at 1698, 1668, and 1562 cm^{-1} in AU, and at 1688, 1548, and 1536 cm^{-1} in IC. It is interesting to note that additional isosbestics are shared only by spectra in the *premelting* region. These occur at 1687, 1646, 1631, and 1571 cm^{-1} in AU, and at 1703, 1675, and 1514 cm^{-1} IC.

The CD of AU and IC was measured at 21 different temperatures between 2 and 72°C. Selected spectra are plotted in Figures 8 and 9. Many bands of both synthetic RNAs exhibit significant premelting shifts in intensity and wavelength. The intensity changes at three different wavelengths are illustrated in Figure 10. In AU, there are isoelliptics shared only by premelting spectra (256 and 288 nm) or only by melting spectra (255 nm). The full range of AU spectra exhibit

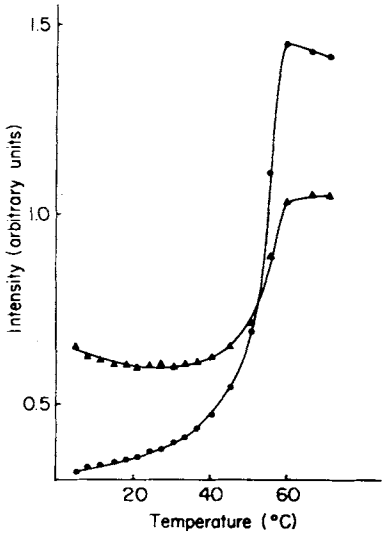

Fig. 6. Intensities of vibrational bands in poly(rI):poly(rC) as a function of temperature: (●) 1659.0 cm^{-1}, (▲) 1505.0 cm^{-1}. Baseline-corrected data. Estimated T_m from both sets of data is 55°C, as compared to a range of values between 55 and 61°C from uv spectroscopy (Ref. 24).

common isoelliptics at 217, 238, and 296 nm. In IC, isosbestic points occur at 219 (premelting only), 265 (melting only), and 256 and 269 nm (all temperatures).

Determination of Thermodynamic Parameters from Spectroscopic Premelting Data

Table III describes the sets of ir and CD data that were analyzed with programs I and II. These include intensities (I) and frequencies (ν) of vibrational bands and CD in molar extinction units (ϵ) at different temperatures. Difference spectra for ir (Fig. 11) and CD (Fig. 12) were calculated by subtracting the spectrum at the lowest temperature of observation from each of the remaining spectra. The intensity (ΔI) of some of the ir difference bands and the differential CD ($\Delta\Delta\epsilon$) of some bands were analyzed with the two programs. In all cases, data were selected from each temperature observed, from the lowest to about 45°C, a point well below the first manifestation of the cooperative helix-coil transition.

Program I was given a wide latitude of guesses for fitting each data set: ΔH^0 between 1.0 and 50 kcal/mol and T_m between -100 and 2000°C. The value 50 kcal/mol was considered a reasonable upper limit because the apparent enthalpy for a highly cooperative transition such as melting is itself in the hundreds of kcal/mol; 2000°C was chosen because it is several times larger than the T_m values calculated from

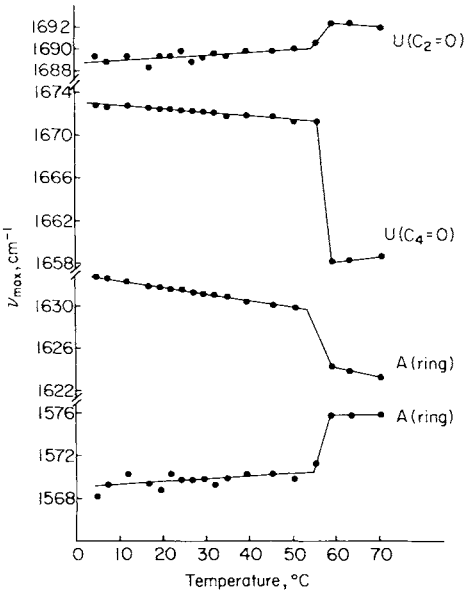

Fig. 7. Frequencies of vibrational bands in poly(rA):poly(rU) as a function of temperature. Baseline-corrected data.

HX data (Table I). If the program selected a pair of values within these extremes, it was rerun using successively narrower ranges of guesses, until the minimizing value of ΔH^0 was determined to the nearest 100 cal/mol and T_m to two significant figures. These results are listed in Table IV. On the other hand, no further iterations were attempted if the first run selected values at one or more of the extreme guesses; for example, $\Delta H^0 = 1.0$ kcal/mol or $T_m = 2000$°C. In these cases, Eq. (3) is minimized by enthalpy or T_m values outside our "reasonable" range. This sort of result is indicated with the appropriate "greater than" or "less than" signs in Table IV.

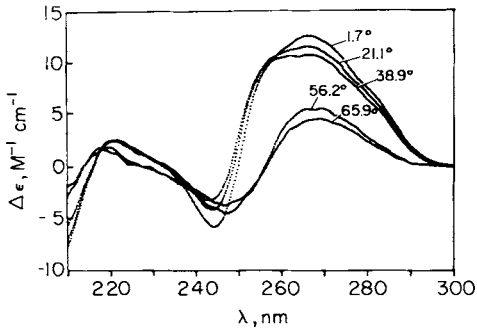

Fig. 8. CD of poly(rA):poly(rU) at different temperatures. The solvent was H_2O, 100 mM NaCl, 1 mM NaH_2PO_4, pH 7.0. Data were corrected for a slight drift in baseline (over 300 nm) with temperature.

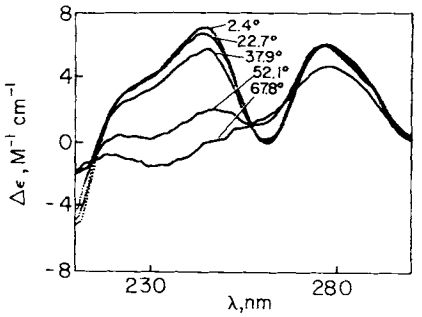

Fig. 9. CD of poly(rI):poly(rC) at different temperatures. Conditions and corrections were the same as those described in the legend to Fig. 8.

According to the above criteria, program I produced a successful minimization with only about one-third of the data sets. The analysis of the K_{op} data from HX (sets 1 and 16) generated enthalpies in close agreement with the values we had calculated from van't Hoff plots (Table I), especially for IC. However, the minimizing value for T_m was over 2000°C.

Program II (see Introduction) incorporates an additional normalizing assumption, specifying a value of $K = K_{ref}$ at $T = T_{ref}$. Equation (4) becomes

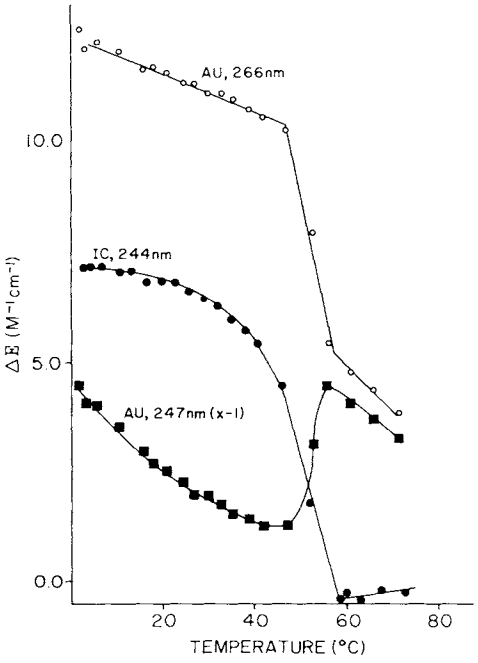

Fig. 10. Intensities of CD bands as a function of temperature. Baseline-corrected data.

TABLE III
Description of Data Sets

	Set Number	Technique	Parameter	Frequency (cm^{-1}) for IR, or Wavelength (nm) for CD
Poly(rA):poly(rU)	1	HX	K_{op} [a]	
	2	ir	I	1690
	3	ir	I	1672
	4	ir	I	1658
	5	ir	I	1624
	6	ir	I	1663
	7	ir	I	1624
	8	ir		1690
	9	ir		1672
	10	ir		1631
	11	ir		1570
	12	CD		244
	13	CD		266
	14	CD		247
	15	CD		266
Poly(rI):poly(rC)	16	HX	K_{op} [b]	
	17	ir	I	1694
	18	ir	I	1659
	19	it	I	1648
	20	ir	I	1505
	21	ir	I	1698
	22	ir	I	1530
	23	CD		244
	24	CD		246

[a] Poly(rA) standard.
[b] Poly(rC) standard.

$$\ln K_{ref} = a/R = -\Delta H^0/RT_{ref} + \Delta S^0/R \quad (6)$$

where a is a constant. Solving for ΔS^0 gives

$$\Delta S^0 = (1/T_{ref}\Delta H^0) - a = b(\Delta H^0) - a \quad (7)$$

where b is another constant; ΔS^0 is now a function of ΔH^0. Thus, only guesses of the enthalpy, again between 1.0 and 50 kcal/mol, were given. The results of fitting the data sets with program II are listed in Table IV. About two-thirds of the sets, including the HX K_{op} data, were successfully fit.

DISCUSSION

Evaluation of Data-Fitting Routines

The analytical methods used to derive thermodynamic parameters from premelting data are based on the assumption of a transition

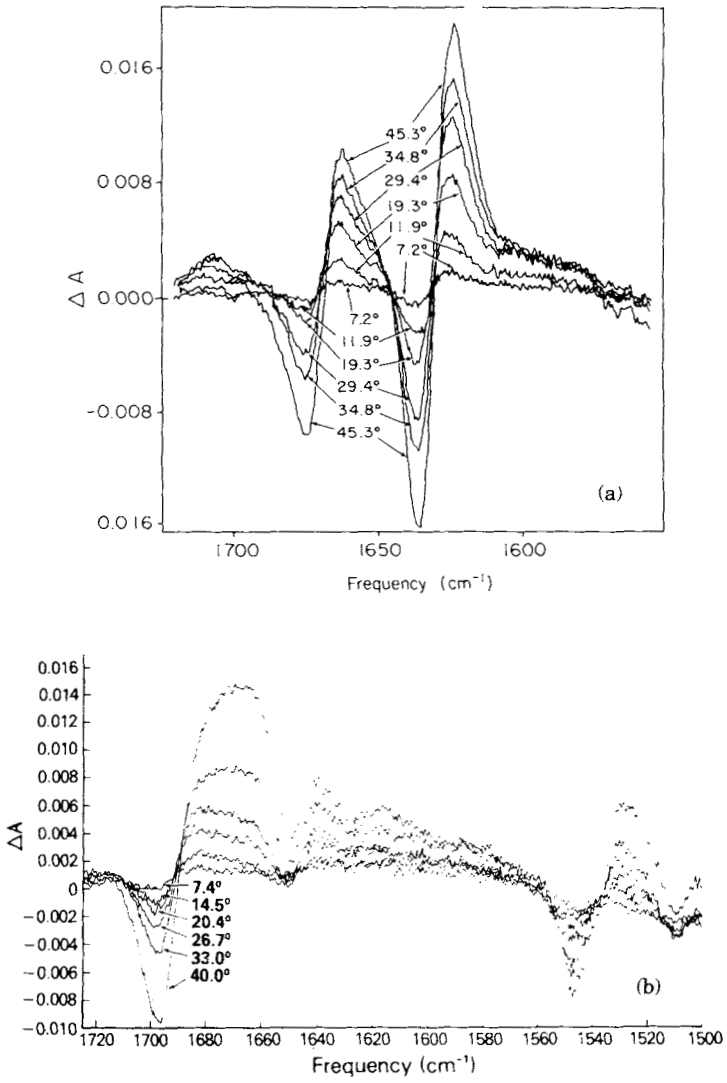

Fig. 11. Infrared temperature-difference spectra: (a) poly(rA) · poly(rU), (b) poly(rI) · poly(rC). For each synthetic RNA, the lowest temperature spectrum was subtracted from each of the other spectra in the premelting range.

between two discrete states. This model is useful in describing the effect of temperature on HX kinetics where the two states represent a base pair unavailable for exchange and an open base pair. Powell and her co-workers[19] found originally that the temperature-dependent conformational change in dinucleoside phosphates, as monitored by CE or uv absorption, could also be treated as a transition between two states fully stacked and unstacked.

In attempting to analyze the ir and CD premelting data, however,

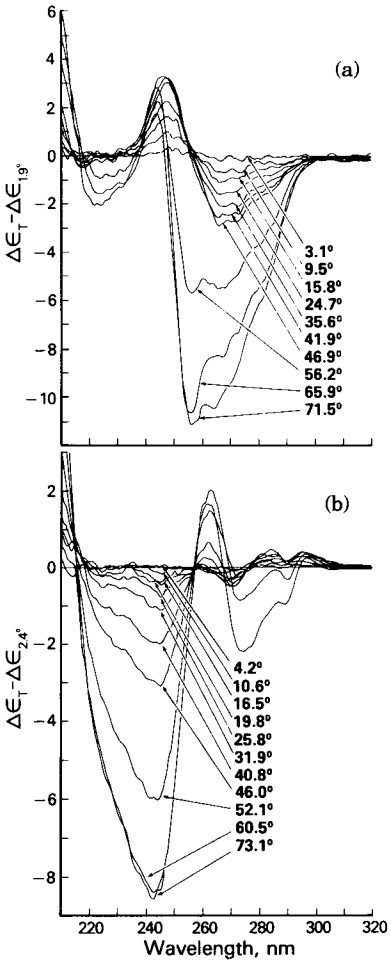

Fig. 12. CD temperature-difference spectra: (a) poly(rA):poly(rU), (b) poly(rI):poly(rC). Procedure was the same as that described for Fig. 11.

we are hindered by the lack of obvious reference states for defining a conformational transition. One reason is that we are uncertain of the nature of the changes detected by spectroscopy, although various possibilities will be explored later in this discussion. Second, whatever "premelting" is, the low-temperature point at which the double helices are totally "nonpremelted" is not known. Davis and his co-workers[11] measured the CD of DNA in high concentrations of LiCl, allowing them to collect spectra at temperatures down to −50°C. They observed that the decrease in amplitude of the long-wavelength positive band leveled off at about −35°C. It appears unlikely that the data from the lowest temperatures in our series, 2°C for CD and 5°C for ir, are close to the lower end of the premelting transition. At higher temperatures, the noncooperative transition is obscured by the highly cooperative

TABLE IV
Results of Computer-Fitting Routines

Set Number	Program I		Program II	
	H^0 (kcal/mol)	T_m (°C)	H^0 (kcal/mol)	T_m (°C)
1	5.5	>2000	6.0	150
2	50	170	34	41
3	16	52	14	69
4	2.0	−100	1.0	−100
5	25	49	26	47
6	2.6	−100	1.0	−100
7	1.0	−100	1.0	100
8	22	39	13	74
9	17	27	1.6	−100
10	1.8	2000	1.7	−100
11	9.4	2000	9.6	93
12	9.4	11	1.0	−100
13	2.3	2000	2.2	2000
14	6.3	−13	1.0	−100
15	1.0	2000	1.0	−100
16	4.3	2000	4.4	510
17	39	44	29	56
18	14	2000	14	96
19	8.9	2000	9.1	150
20	50	37	46	44
21	17	2000	18	79
22	7.0	2000	7.3	200
23	14	2000	14	95
24	14	2000	14	96

process of denaturation. Although the T_m for the helix-coil transition in Au and IC is in the range of 55–60°C, the HX measurements between 10 and 40°C extrapolate to apparent T_m values between 200 and 900°C for localized base-pair openings (Table I). A number of spectroscopic data sets also yield T_m values greater than denaturing temperatures (Table IV), although we consider these to be less reliable than the H^0 values, as will be discussed later. It cannot be assumed that the "fully premelted" molecules have the same conformation or spectrum as the random coil. Hence we cannot use the latter as a reference state for the premelting transition.

Program I computes values of the spectral parameters, α_A and α_B [Eq. (1)], corresponding to the pure states, A and B, at the two endpoints of the transition. A van't Hoff line is calculated for each of the combinations of input guesses of ΔH^0 and T_m. Each van't Hoff equation generates values of the spectroscopic parameter; $\alpha^* T$, for each of the observation temperatures. The α_T values are compared to the experimental α_T until the combination of guesses producing the minimum sum of squares [Eq. (3)] is identified.

The minimization procedure may fail or generate anomalous results

if the experimental data deviate greatly from the form of a van't Hoff line. Such a problem could arise if (1) the parameter, α, is not sufficiently temperature-dependent,[19] (2) the data are excessively noisy, (3) the data represent a transition among more than two states or more than one transition, or (4) the transition is cooperative. To some extent, the last alternative is refuted by the gradual nature of the apparent spectral changes over a broad temperature range. However, a residual weak cooperativity cannot be excluded. The third possibility cannot be addressed because of our limited understanding of premelting. The first two alternatives are difficult to assess by inspection of the experimental data because in the course of the fitting routine, the data are transformed into coordinates of ln K and $1/T$ via operations dependent on unknown values of ΔH^0 and T_m. Some of the data sets that seemed to be noisy were successfully fit by program I; some of the "cleanest" sets, such as the intensities at 1624 cm^{-1} in the ir spectrum of AU (Fig. 5; data set 5 in Table IV) were not.

In program II, ΔS^0 (and T_m) becomes a function of ΔH^0 [Eq. (7)], meaning that the y-intercept of a van't Hoff line is determined by its slope. Consequently, the range of possible fits to a data set is greatly reduced. Since the 20°C point is fixed at a low value of K_{eq} (0.05 for AU and 0.01 for IC), and the experimental temperatures are clustered closely around 20°C (especially in the $1/T$ transform), the likelihood of minimization by outlandish values of ΔH^0 (and T_m, a function of ΔH^0) is diminished. Nevertheless, the failure of program II with one-third of the data sets suggests that this scheme is still sensitive to large deviations from ideal behavior by the experimental points.

The imposition of values of K_{eq} derived from HX on spectroscopic data is, of course, arbitrary and raises questions about the validity of these fits. However, examination of Table IV reveals a striking correlation between enthalpies generated by programs I and II. In a number of cases, applying the normalizing assumption brings T_m inside our limits without significantly affecting ΔH^0. Because of the wide discrepancies between T_m values produced by the two programs, and the dependence of T_m on ΔH^0 in program II, we do not place much weight on interpretation of T_m (or ΔS^0) figures. Enthalpies generated by program I were selected for further consideration if they fulfilled one of the following criteria: (1) the values for a data set derived from programs I and II were similar to within 10% and the T_m derived from either program was within the assigned limits, and/or (2) both ΔH^0 and T_m values derived from program I were within the assigned limits. These enthalpy data of reasonable confidence are listed in Table V.

Premelting and Melting Transitions

A number of observations and theoretical considerations suggest that the premelting reported here and in the literature is distinct from the helix-coil transition.

TABLE V
Calculated Enthalpies of Premelting Transitions

	Technique	Number of data sets	H^0 (kcal/mol)
Poly(rA):poly(rU)	HX	1	3.8[a]
			6.1[b]
			5.5[c]
	ir	5	16
			25
			22
			17
			9.4
			(Average) 18 ± 5.4
	CD	2	9.4
			6.3
			(Average) 7.9
Poly(rI):poly(rC)	HX	1	3.7[a]
			6.3[a]
			4.3[c]
	ir	5	39
			14
			8.9
			17
			7.0
			(Average) 17 ± 11
	CD	2	14
			14
			(Average) 14

[a] From van't Hoff plot based on Eq. (1); polynucleotide standard.
[b] From van't Hoff plot based on Eq. (1); mononucleotide standard.
[c] From program I; polynucleotide standard.

Ultraviolet hyperchromicity is considered to be a sensitive monitor of double-helix denaturation. Our measurements (data not shown), in agreement with previous work,[21,25] show essentially no uv absorbance change until five degrees below the T_m, or over 50°C, in both AU and IC. Temperature effects on HX kinetics as well as in ir and CD spectral bands are, of course, prominent at much lower temperatures.

Denaturation is a highly cooperative transition with an apparent enthalpy change in the range of hundreds of kcal/mol. Premelting, on the other hand, is characterized by ΔH^0 values between about 5 and 20 kcal/mol, depending on the technique of measurement (Table V). The cooperative unit for the CD-detected premelting of poly[d(A—T)] appears to be less than 10 base pairs.[7]

In DNA and poly[d(A—T)] the long-wavelength positive CD band increases in the premelting region but decreases through the melt,[5-7,9] consistent with the occurrence of a distinct process over the

lower range of temperatures. A similar reversal is seen in the short-wavelength negative CD band in AU (Figs. 8 and 10).

Existence of an isosbestic point is a necessary but not sufficient condition for a transition between two conformations,[18] such as helix and coil. The existence of isosbestics in the ir and CD spectra of AU and IC that are unique to premelting spectra is thus consistent with the hypothesis that a transition between intermediate conformations occurs prior to the onset of denaturation.

The helix–coil transition in polynucleotide duplexes is sensitive to monovalent cation concentration; the T_m of AU increases by 36°C, for example, when Na^+ is raised from 0.01 to 1*M*. However, the same change in Na^+ has no effect on the kinetics or equilibrium of base-pair opening, as detected by HX.[17] Another measure of premelting change, the increase in the long-wavelength CD band in DNA and poly[d(A—T)], also is insensitive to a 100-fold increase in Na^+.[7]

Gralla and Crothers[26] estimated a probability of 10^{-10} for concerted opening of nine A:U base pairs in a long RNA double helix at 25°C. In their model, the A:U region is bounded by G:C pairs. Thus, the probability should be slightly higher in AU. However, formation of an analogous denatured bubble in IC should be considerably less likely. In contrast to these predictions, we observed from HX that 0.05 of the base pairs in AU and 0.01 in IC are open at 25°C. The relatively high frequency of observed openings at this temperature must be accounted for by localized opening of the helical structure, rather than by co-operative denaturation of such a large proportion of the duplex. The fraction of base pairs involved in spectroscopically observed premelting changes is extremely difficult to determine absolutely with any precision. But the fact that both IR and CD can detect these phenomena implies that they also must be far more probable than denatured bubbles.

Interpretation of Premelting Changes in IR and Raman Spectra

No previous studies of premelting using ir absorption spectroscopy have been published, but several workers have reported low-temperature changes with Raman scattering.[12–14] Although the selection rules for ir and Raman transitions are different, the two techniques produce a number of similar bands in large asymmetric molecules such as polynucleotides. Small and Peticolas[12] found, in the Raman spectrum of AU in D_2O, uracil carbonyl and adenine ring vibration bands at frequencies close to the corresponding ir bands. Upon melting, a Raman band appears at 1660 cm^{-1} analogous to the uracil C4 carbonyl band at 1658.5 cm^{-1} in the ir. In both cases, there is a premelting increase in intensity, much smaller in magnitude but in the same

direction as the melting hyperchromism. Because of the sensitivity of the uracil carbonyl bands to hydrogen bonding,[18] their premelting change in the Raman band is ascribed to a gradual "loosening" of the native hydrogen-bonded structure.[12] On the other hand, the frequency shift of the uracil carbonyl band in the ir (Fig. 7), which parallels strikingly the behavior of a thymine carbonyl Raman band in DNA,[13] implies that unstacking of bases, as well as hydrogen-bond breakage, may account for premelting in this spectral region.

Small and Peticolas[12] do not indicate whether the adenine ring vibration band at 1623–1631 cm^{-1} in the Raman spectrum of AU shows premelting effects. However, they present data for the ring vibration bands at 1236 (uracil) and 730 cm^{-1} (adenine), in H_2O solvent. Both bands increase with temperature, consistent with base unstacking. In the ir spectrum, there are analogous hyperchromic premelting and melting changes at 1624 cm^{-1} (adenine ring vibration, Fig. 5). Unstacking here is accompanied by a large blue shift (Fig. 7), as is also observed in the uracil Raman band (1238 cm^{-1}).

Parallel premelting changes are seen in the ir spectrum of IC. The hypoxanthine and cytosine carbonyl vibrations occur, respectively, at 1695 and 1648 cm^{-1} in the low-temperature spectrum (Fig. 4 and Table II). These shift either to the red (hypoxanthine) or the blue (cytosine), forming, in the denatured spectrum, a broad band with a peak at 1659 cm^{-1}, and an asymmetric profile leaning toward higher frequencies (wave numbers). This band is a summation of the poly(rI) (1673 cm^{-1}) and poly(rC) (1656 cm^{-1}) vibrations.[27] The low-temperature band at 1543 cm^{-1} includes contributions from both hypoxanthine and cytosine ring vibrations, with the latter predominating. As the bases unstack, this band shifts to the red (1522 cm^{-1} in the denatured spectrum) and increases in intensity. The band at 1505 cm^{-1} also is a combination of a large cytosine band [1504.5 cm^{-1} in poly(rC)] and a smaller hypoxanthine band [1507 cm^{-1} in poly(rI)].[27] Perhaps because of its complexity, this band displays the unusual behavior of a decrease in intensity in the premelting region followed by hyperchromism during the melt (Fig. 6). Its frequency does not change over the entire temperature range of observation.

The Raman band at 814 cm^{-1} in AU (H_2O solvent) has been assigned to the symmetric stretching of the phosphodiester group.[12] Its intensity decreases over a wide range of temperatures, implying a gradual loss of the native ordered structure of the backbone during the premelt followed by an abrupt cooperative transition to the random coil.

Interpretation of Premelting Changes in CD Spectra

There have been a number of reports demonstrating premelting changes in the CD spectra of DNA and synthetic deoxyribopolymer

duplexes.[5-11] The intensity of the long-wavelength positive band (around 278 nm in DNA and 262 nm in poly[d(A—T)]) increases with temperature in the premelting region, but decreases upon denaturation. The negative band at about 247 nm increases through both premelting and melting. Davis and his co-workers found that reducing the ionic strength at a constant temperature produced the same effects on the CD as did raising the temperature in the premelting region.[11] Experiments with closed circular superhelical DNA[28] showed that either of these environmental changes decreases the winding angle of the double helix. Consequently, several authors have attributed the premelting CD effects to a reduction in the helix winding angle (σ or τ), or equivalently, to an increase in the number of base pairs per turn.

Among the major DNA structures characterized by x-ray diffraction, winding-angle decrease has been observed to follow the order C > B > A.[15] Brahms and his co-workers compared their premelting spectra of poly[(A—T)] in Na^+ solution to a Li^+ film spectrum at 82% relative humidity, conditions in which ir dichroism indicated the C-helix.[5] By extrapolation of CD intensity measurements, they calculated that a 100% C spectrum would occur in Na^+ solution at -80°C. Thus, they interpreted premelting as the transition from the C- to B-form, a view shared by Greve et al.[8] Gennis and Cantor[7] argue against this conclusion on the grounds that DNA is more hydrated at lower temperatures, whereas the C-helix is associated with partial dehydration. Recent fiber-diffraction studies[29] have demonstrated that DNA occurs in the B-form even at the highest salt concentrations (and presumably at the lowest temperatures) employed by authors of previous studies. The C-form is observed under certain drastic conditions that produce dehydration, but is unlikely to be involved in the premelting transition normally observed.

Gennis and Cantor[7] regard a B–A-helix transition as an even less-likely explanation of CD premelting than the B–C conversion. The former process is expected to show a higher enthalpy than their estimate of 5 kcal/mol or less. They also predict a dependence on ionic strength for ΔH^0 B–A, but observe no effect of Na^+ concentration. Finally, glucosylated $T2r^+$ phage DNA, which cannot assume the A-form (at least not in films), exhibits premelting. A last piece of evidence against a B–A transition comes from Raman spectroscopy of DNA solutions.[13]

Johnson et al.[15] found that the CD intensity at 275 nm was sensitive not only to variations in winding angle, but also to the tilt of the base pairs from the helix axis, the twist of the bases, the displacement of the base pairs from the helix axis, and the step height; that is, all the parameters needed for a unique assignment of the bases' relative positions. In this study, the CD spectrum was calculated for 68 different conformations of an 11-base-pair DNA, including structures deduced

from fiber-diffraction measurements (the A^-, B^-, B'^-, C^-, and D-helices), theoretical minimum-energy forms, and variants of the first two categories generated by thermal fluctuations in tilt and twist. The intensity at 275 nm was most strongly correlated with winding angle and twist. All the parameters, except step height, were found to be linked. Thus, earlier interpretations of CD premelting in terms of decreased winding angle are probably oversimplified in terms of the conformational change that is actually occurring.

Some authors have suggested a connection between premelting changes in helical structure and temperature effects on hydration of nucleic acid polymers. It has been reported[11] that the slope of the premelting intensity increase at 276 nm in DNA shows a strong positive correlation with the heat of hydration of the solvent cation ($Li^+ > Na^+ > K^+ > NH_4$). The authors propose that temperature-dependent changes in the hydration of cations bound to or near DNA phosphates affect the backbone conformation. Similar factors are invoked by DeMurcia et al.[6] to explain the reduction in T_m and CD premelting changes in the presence of tetramethylammonium (TMA^+) ions, which are less hydrated than alkaline cations. However, these authors must also include a specific binding of TMA^+ to A:T pairs as part of their hypothesis.

Is it possible to apply the results and conclusions from CD-premelting studies of DNA to our observations on RNA double helices? In DNA and poly[d(A—T)], the positive long-wavelength band increases with temperature, while in AU, it decreases (Ref. 30 and this work—Figs. 8 and 10) and in IC remains constant (Fig. 9). In IC, there is a shorter-wavelength positive band which *does* decrease in the premelt (Figs. 9 and 10). Double-stranded RNAs are prevented, by the bulk of the 2'-OH group, from assuming the B- or C-helix.[31] The structure that agrees best with diffraction measurements, RNA-11, has 11 base pairs per turn, as does A-DNA. Another possible model is RNA-10, with the same winding angle as B-DNA, but with a tilt closer to that of A-DNA.[31] In DNA, the intensity of the long-wavelength positive band decreases from the A family, characterized by a smaller winding angle (larger number of base pairs per turn), larger twist angle, and negative tilt, to the B family.[15] By analogy, AU and IC may show a decrease in CD intensity in the premelt due to a transition between a conformation similar to RNA-11, and one closer to RNA-10, exhibiting a larger winding angle and a less negative tilt. It is interesting to note that the same sort of temperature dependence described for the DNA positive band is displayed by the *negative* band at shorter wavelengths (244–247 nm) in AU (Figs. 8 and 10). The interpretation of premelting in this band, like the analogous band in DNA, is rather unclear.[15]

In contrast to the opposite trends seen in the premelting region, the long-wavelength positive bands in both DNA[5–8,10] and RNA (Ref. 30 and this work—see Figs. 8–10) decrease in the helix–coil transition.

In each case, the band also experiences a red shift upon melting. The fact that these trends are common to DNA and RNA is consistent with the view that the cooperative denaturation of both types of double helices is, at least qualitatively, similar.

Comparison of Spectroscopic Premelting with HX-Detected Opening

Premelting changes in the Raman spectrum of AU[12] and calf-thymus DNA,[13,14] are generally in the same direction; that is, increasing or decreasing intensity, red- or blueshift, as the corresponding changes during melting. We have found this same pattern in most of our ir data, with the notable exception of the 1505 cm^{-1} band in IC (Fig. 6). With DNA, the similarity in trends between premelting and melting contrasts with the trend reversal observed in CD spectra. Premelting changes in the Raman bands appear to be caused by partial unstacking and hydrogen-bond breakage. Since these processes continue during cooperative denaturation, it is not surprising that the spectral changes are in the same direction, but larger in magnitude. On the other hand, premelting effects observed by CD have been attributed to small changes in the winding angle and associated helical parameters. Since the collapse of the ordered structure upon denaturation involves both unstacking of bases and hydrogen-bond breakage, there is no reason to predict a spectral effect in the same direction as premelting. According to this view, it may be a coincidence of unrelated factors that results in CD melting-intensity changes in the same direction in RNA, but in different directions in DNA.

The CD premelting data for IC could support an interpretation different from the one based on DNA studies. Unlike the component polyribonucleotides in AU, poly(rI) and poly(rC) have markedly different CD spectra.[32] Comparing these to the spectrum of IC leads to the tentative assignment, in the latter (see Fig. 9), of the positive band at 244 nm to hypoxanthine–hypoxanthine stacking interactions, and the positive band at 277 nm to cytosine–cytosine stacking. Poly(rI) forms a quadruple-helical complex in high salt at low temperatures.[33] The premelting decrease in the 244 nm band (Fig. 10) might then reflect an opening of regions in the double helix and exposure of inosinic residues to the solvent, followed by intramolecular complex formation and disruption at higher temperatures. According to this hypothesis, the lack of premelting change in the 277-nm band would be due to the inability of cytidylic residues to associate.

There are several difficulties that arise from the hypothesis just presented. It has been argued previously that any low-temperature base-pair opening detected by our methods must occur in very short units. It may not be possible for isolated open inosinic residues to form a complex. Also, if CD is sensitive to the small amount of opening in

IC (1% from HX measurements), one might expect the 277-nm band to change as exposed cytosines unstack. Both hypoxanthine and cytosine vibrational bands in the ir spectrum do show premelting changes consistent with unstacking.

It has been suggested that the ir spectral effects observed in the premelting region are related to some sort of localized disruption of the native structure. If ir is monitoring base-pairing opening, then the enthalpy associated with changes in the vibrational bands should be equal to the enthalpy derived from HX measurements. However, the average ΔH^0 calculated from the ir data is about three times larger than any of the values determined from HX in both AU and IC (Table V). It is improbable that another frequent mode of opening could exist undetected by HX measurements.[17] Therefore, a more likely conclusion is that ir measurements are hardly affected by the open state detected by HX, but rather are dominated by a set of other conformational changes that do not cause exchange of protons although they determine the enthalpy of the ir premelting transition.

For example, a minimal model proposed for the open state in AU involves a swinging out of the uracil base while keeping the adenine stacked.[17] An alternative model, postulating motile solitons, now seems less likely in view of recent HX data on oligonucleotides.[34] Ir might monitor these perturbations in some small way, but will still be determined by other deformations that involve, for example, unstacking of the adenine, and further excursions of the uracil, which do not effect any (additional) HX.

While the averages of the enthalpies obtained from ir measurements are quite similar for the two synthetic RNAs, CD spectroscopy yields a much larger H^0 in IC than in AU (Table V). The greater temperature dependence of the short-wavelength positive band in IC (both measurements listed in Table V are derived from that band—see Table IV) may reflect a conformation change of a character different from the transition measured by CD in AU. The fact that the enthalpy for CD premelting in IC approaches the average value from ir measurements is consistent with the alternate hypothesis previously discussed. On the other hand, it is possible that the same process could produce spectral effects of a different magnitude in the two synthetic RNAs, just as uv hyperchromicity is sequence-dependent.

Small changes in winding angle and other helical parameters have been invoked to explain CD premelting in DNA, and this hypothesis is perhaps applicable to the RNA data, as well. This type of conformational effect would be expected to involve a smaller enthalpy than base-pair opening, provided that the units participating in each process are equal in size. But Table V shows a slightly larger average enthalpy for CD, compared to HX, measurements in AU. The average ΔH^0 values for CD premelting in AU fall within the range of literature estimates from data on poly[d(A—T)].[5,7] It is possible, then, that CD

monitors a change in winding angle, twist, etc., involving relatively large stretches of nucleotides, but which is insensitive to the opening of isolated base pairs.

These tentative conclusions on the relationship between premelting phenomena detected by HX, ir, and CD can be tested by further investigations with different polymers and different conditions of salt and pH. These studies are in progress.

This research was supported by Grants CA 31207 and GM 29272 from the NIH, and NSF Grant PCM 0-04043.

References

1. Poland, D. & Scheraga, H. A. (1970) *Theory of Helix-Coil Transitions in Biopolymers*, Academic, New York.

2. Fritzsche, H. (1982) *Comm. Mol. Cell. Biophys.* **1**, 325–336.

3. Palacek, E. (1976) *Prog. Nucl. Acid Res. Mol. Biol.* **18**, 151–213.

4. Bezdekova, A. & Palacek, E. (1972) *Stud. Biophys. (Berl.)* **34**, 141–149.

5. Brahms, S., Brahms, J. & Van Holde, K. E. (1976) *Proc. Natl. Acad. Sci. USA* **73**, 3453–3457.

6. De Murcia, G., Wilhelm, B., Wilhelm, F. S. & Daune, M. P. (1978) *Biophys. Chem.* **8**, 377–383.

7. Gennis, R. B. & Cantor, C. R. (1972) *J. Mol. Biol.* **65**, 381–399.

8. Greve, J., Maestre, M. F. & Levin, A. (1977) *Biopolymers* **16**, 1489–1504.

9. Sarocchi, M.-T. & Guschlbauer, W. (1973) *Eur. J. Biochem.* **34**, 232–240.

10. Sprecher, C. A. & Johnson Jr., W. C. (1982) *Biopolymers* **21**, 321–329.

11. Studdert, D. S., Patroni, M. & Davis, R. C. (1972) *Biopolymers* **11**, 761–779.

12. Small, E. W. & Peticolas, W. L. (1971) *Biopolymers* **10**, 1377–1416.

13. Erfurth, S. C. & Peticolas, W. L. (1975) *Biopolymers* **14**, 247–264.

14. Rimai, L., Maher, V. M., Gill, D., Salmeen, I. & McCormick, J. J. (1974) *Biochim. Biophys. Acta* **361**, 155–165.

15. Johnson, B. B., Dahl, K. S., Tinoco, Jr., I., Ivanov, V. I. & Zhurkin, V. B. (1981) *Biochemistry* **20**, 73–78.

16. Preisler, R. S., Mandal, C., Englander, S. W., Kallenbach, N. R., Howard, F. B., Frazier, J. & Miles, H. T. (1981) in *Biomolecular Stereodynamics I*, Sarma, R. H., Ed., Adenine, New York, pp. 405–415.

17. Mandal, D., Kallenbach, N. R. & Englander, S. W. (1979) *J. Mol. Biol.* **135**, 391–411.

18. Miles, H. T. (1971) in *Procedures in Nucleic Acid Research*, Vol. 2, Cantoni, G. L. & Davies, D. R., Eds., Harper and Row, New York, pp. 205–232.

19. Powell, J. T., Richards, E. G. & Gratzer, W. B. (1972) *Biopolymers* **11**, 235–250.

20. Englander, J. J., Kallenbach, N. R. & Englander, S. W. (1972) *J. Mol. Biol.* **63**, 153–169.

21. Wang, A. C. & Kallenbach, N. R. (1971) *J. Mol. Biol.* **62**, 591–611.

22. Nakanishi, M. & Tsuboi, M. (1978) *J. Mol. Biol.* **124**, 61–71.

23. Miles, H. T. (1961) *Proc. Natl. Acad. Sci. USA* **47**, 791–802.

24. Szybalski, E. H. & Szybalski, W. (1975) in *Handbook of Biochemistry and Molecular Biology*, 3rd ed., *Nucleic Acids, Vol I*, Fasman, G. D., Ed., Chemical Rubber Co., Cleveland, pp. 575–588.

25. Stevens, C. L. & Felsenfeld, G. (1964) *Biopolymers* **2**, 293–314.

26. Gralla, J. & Crothers, D. M. (1973) *J. Mol. Biol.* **78**, 301–319.

27. Miles, H. T. (1975) in *Handbook of Biochemistry and Molecular Biology*, 3rd ed., *Nucleic Acids, Vol. I*, Fasman, G. D., Ed., Chemical Rubber Co., Cleveland, pp. 604–623.

28. Wang, J. C. (1969) *J. Mol. Biol.* **43**, 25–39.
29. Zimmerman, S. B. & Pheiffer, B. H. (1980) *J. Mol. Biol.* **142**, 315–330.
30. Hashizume, H. & Imahori, K. (1967) *J. Biochem.* **61**, 738–749.
31. Cantor, C. R. & Schimmel, P. R. (1980) *Biophysical Chemistry, Part I—The Conformation of Biological Macromolecules*, W. H. Freeman and Co., San Francisco, pp. 183–184.
32. Borer, P. N. (1975) *Handbook of Biochemistry and Molecular Biology*, 3rd ed., *Nucleic Acids, Vol I*, Fasman, G. D., Ed., Chemical Co., Cleveland, pp. 592–594.
33. Miles, H. T. & Frazier, J. (1978) *J. Am. Chem. Soc.* **100**, 8037–8038.
34. Englander, S. W. & Kallenback, N. P., (1984) *Q. Rev. Biophys.* **16**, 521–655.

Received August 10, 1983
Accepted February 29, 84